Journal of Mechanical Engineering *Vol SI 4(2), 249-267, 2017*

Wireless Condition Monitoring System for Rotating Machinery Powered by a Hybrid Vibration Based Energy Harvester

Mohd Sofwan Mohd Resali[*]*, Hanim Salleh*
Institute of Sustainable Energy,
Universiti Tenaga Nasional (UNITEN)

[*]*mohdsofwan@gmail.com*

ABSTRACT

This paper presents the development of wireless condition monitoring system for rotating machinery powered by a hybrid vibration based energy harvester. The self-powered condition monitoring system consists of three parts. The first part of the system is the energy harvester, the second part is the power management and the third part is the android based user interface. The system used a hybrid energy harvester (piezoelectric and electromagnetic) to harvest energy from the vibrating machine at a resonance frequency of 50±2 Hz and 0.25g ms^{-2} *of acceleration. The maximum output power from the hybrid harvester was 3.00 mW at 200 kΩ of load resistor. The power management circuit efficiency was 85% with output power of 2.55 mW. An accelerometer sensor and a temperature sensor were connected to the power management unit to sense the vibration and temperature level of the machine. Data from the sensors were transmitted through the wireless Bluetooth dongle to the android phone for end user monitoring. An android application was developed to receive the acceleration and temperature condition monitoring. At maximum power, initial charging duration of the supercapacitor was 130 seconds, and duration for recharging to 8.2V was 15 seconds. Therefore, the self-powered system managed to transmit data to the android application 15 second's intervals.*

ISSN 1823- 5514, eISSN 2550-164X
Received for review: 2017-04-30
Accepted for publication: 2017-06-07
Published: 2017-09-15

Keywords: *vibration, energy harvesting, condition monitoring, hybrid*

Introduction

Recent designs in power electronics and sensors have been modified towards low power consumption in the range of micro and milliwatts [1, 2]. Due to this, there are promising potential application of energy harvesting technology as the source of power. Some of the application of energy harvesting technology are for the wireless medical implants [3, 4], wireless sensors and similar structures are just a few of many examples [5]-[7].

One of the source of energy harvester is from vibration, which converts mechanical energy to electrical energy. Vibration energy harvesting can be harvest by using three types of transduction, which are the electromagnetic, [8]-[13], piezoelectric [PZT] and electrostatic. Researcher start to explore on the electromagnetic energy harvester and characterize the performance of the harvester. People also look for a study on the electrostatic energy harvester [14]-[18] to generate power from the vibration. Most of the reports shows the output power generated from the electrostatics energy harvester are low compare to the electromagnetics and piezolectric energy harvester. Pieozoelectric energy harvester by using piezoelectric material also were used to harvest energy from the vibration energy harvesting [19]-[26]. People start to sudy from the literature to the improvement of the output power by proposed a few techniques and strategy.

The other important point to focus besides improvement of the energy harvester itself is the application on what can be done from the output power from vibration energy harvesting. Not many researcher focus on the application works of the energy harvesting. One of the applications can be used by applying energy harvesting is the condition monitoring system powered by piezoelectric and electromagnetic energy harvester. Jae Hyuk Jang et al. [27] proposed a wireless condition monitoring system powered by 100μW vibration based energy harvester from piezoelectric. It is proposed by using wireless sensor networks (WSN) technique by using 85 nodes to reduce the power consumption excited at 0.45g ms^{-2} of acceleration and 40.5 Hz of resonance frequency. The end user can monitor the condition monitoring by acces it at the base station. L. Chen et al. [28] also proposed the condition monitoring system powered by piezoelectric energy harvester. The system excited at 0.9g ms^{-2} of the acceleration and at 44 Hz of the resonance frequency.

This paper proposed a condition monitoring system powered by hybrid energy harvester (HEH) with combining piezoelectric and electromagnetic energy harvester. The system excited at 0.25g ms^{-2} of the acceleration and 50 Hz of resonance frequency. This condition monitoring system proposed the HEH as power source and transfer the energy to the

power management unit to power up the microcontroller, sensors with wireless communication module and transfer the sensors data to the android phone. This paper proposed the bluetooth communication type as a wireless device. The details of the system design and architecture of the condition monitoring system is described in the next section below.

System design and architecture

The system design and architecture of the self-powered condition monitoring system is shown in Figure 1. This architecture consists of three parts. The first part of the system is the energy harvester, the second part is the power management and the third part is the user interface. The hybrid energy harvester will convert energy from the vibrating machine into electrical energy to the system. The electrical energy then is transferred to the second part of the condition monitoring system. This second part consists of a few components with the power management circuit, microcontroller, sensors and wireless communication module. The last part is the android phone with the graphical user interface (GUI) installed inside the android phone to receive the data send from the second part via wireless communication module. Next section describes in detail each of the components of the system.

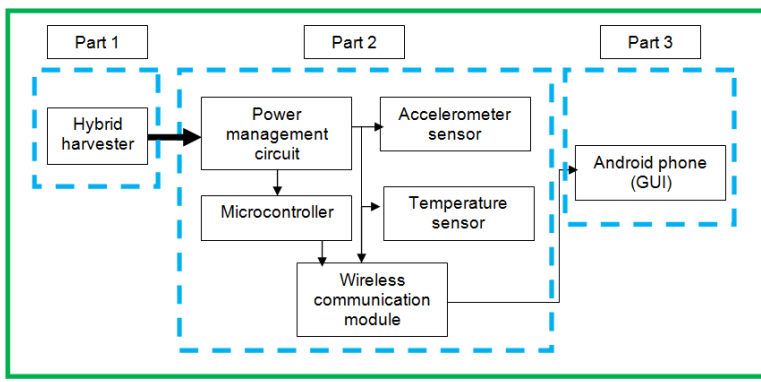

Figure 1: System design and architecture for the acceleration and temperature condition monitoring system

Part 1: Energy harvester

Hybrid energy harvester (HEH) as shown in Figure 2 is designed by combining piezoelectric and electromagnetic energy harvester; to convert from mechanical energy to the electrical energy. The resonance frequency of the HEH is fixed at 50±2 Hz and 0.25g ms^{-2} of the acceleration.

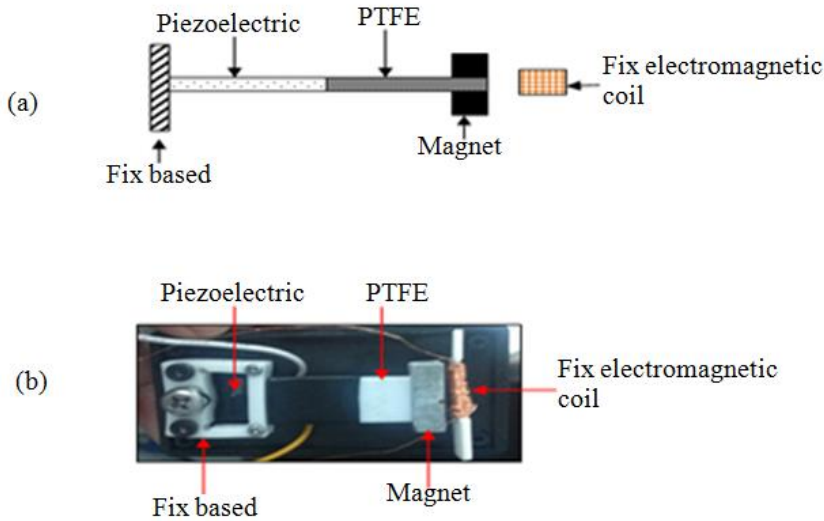

Figure 2: Hybrid energy harvester

The extension of PTFE beam is connected to the end of the piezoelectric harvester as portrayed in Figure 2 (a) in order to work at the desired working frequency. The power output of the piezoelectric harvester, P_{piezo} can be calculated in Equation (1):

$$P_{piezo} = \frac{1}{2} I^2 Z_L = \frac{1}{2} \frac{(V_{OC})^2}{(2Z_S)^2} (Z_S) = \frac{1}{4} \frac{V_{OC}^2}{Z_S} \tag{1}$$

Where V_{OC} is the open circuit voltage (Volt) of the piezoelectric harvester and Z_s is the optimal load resistance (Ohm). The V_{OC} can be calculated in Equation (2):

$$\begin{aligned} V_{OC} &= -\frac{E_{piezo}}{K} \frac{h_{piezo}}{L_{piezo}} \int_0^{L_{piezo}} S(x) dx \\ &= \frac{6E_{piezo}}{K} \frac{h_{piezo}(h_{piezo} + h_{ptfe}/2)}{L_{piezo}^2 (L_{piezo} + 3L_{ptfe})} \left(\frac{1}{2} (L_{piezo}) + L_{ptfe} \right) \alpha \end{aligned} \tag{2}$$

Where E_{piezo} is the elastic modulus (N/m^2) of the piezoelectric, K is the dielectric constant of the piezoelectric, L_{piezo} is the length (mm) of the piezoelectric, h_{piezo} is the thickness (mm) of the piezoelectric, h_{ptfe} is the thickness (mm) of PTFE material, L_{ptfe} is length (mm) of the PTFE material and α (mm) is the deflection of the piezoelectric. According to the maximum power transfer theorem, the maximum power occurs when the load impedance is equal to the source impedance.

The basic equation of the electromagnetic energy harvester is based on the Faraday's law of electromagnetic induction as described in Equation (3):

$$V_{emc} = -\frac{d\phi}{dt} \tag{3}$$

In which V_{emc} (V) is the voltage induced at the conductor and is proportional to the rate of change of the magnetic flux ϕ (Wb) of the circuit. In the actual electromagnetic energy harvester using fixed permanent magnet, the V_{emc} generated by the coil is expressed as Equation (4), where N is the number of turns and ϕ is the average flux:

$$V_{emc} = -N\frac{d\phi}{dt} \tag{4}$$

The power generated by the electromagnetic energy harvester is measured by connecting the load resistance R_L (Ohm) to the harvester. In the frequency domain, the output power, P_{emc} (Watt) of the electromagnetic generator can be expressed from Equation (5) to Equation (7) as below:

$$P_{emc} = \frac{m_{emc}\omega_{emc}^3 Y_{emc}}{16\xi_{emc}}\left(\frac{R_L}{R_L + R_i}\right) \tag{5}$$

$$\xi_{emc} = \frac{NL_{emc}\phi}{2m\omega_{emc}\left(R_L + R_i\right)} \tag{6}$$

$$R_i = \frac{8\rho\left(d_0 + d_i\right)N^3}{\left(d_0 + d_i\right)^2} \tag{7}$$

In Equation (5), Equation (6) and Equation (7) m_{ec} is the mass (gram), ω_{ec} is the resonance frequency (rad/sec), R_i is the coil resistance (Ohm), R_L is

the load resistor (Ohm), ζ_{ec} is the damping ratio, ρ is the resistive coil material d_o is the coil outer diameter (mm) and d_i is the coil inner diameter (mm). Theoretically, the total output power of the HEH, P_{HEH} is the sum of the output power of both mechanisms as summarized in Equation (8).

$$P_{HEH} = P_{piezo} + P_{emc} \tag{8}$$

Part 2: Power management circuit and microcontroller

Power management circuit

The hybrid harvester (HEH) produces AC voltage that go to the power management circuit as illustrated in Figure 3. The AC-DC rectifier rectifies the input AC voltage from the HEH to the DC voltage prior transfer it out to the voltage clamp circuit. Here, the zener diode is added and set up at the maximum 10V DC voltage for circuit protection. The supercapacitor storage circuit stored the input voltage until it is fully charged, before it starts to flow the energy to the DC-DC up or down converter circuit. The switching circuit is ON and OFF to control the energy stored in the supercapacitor.

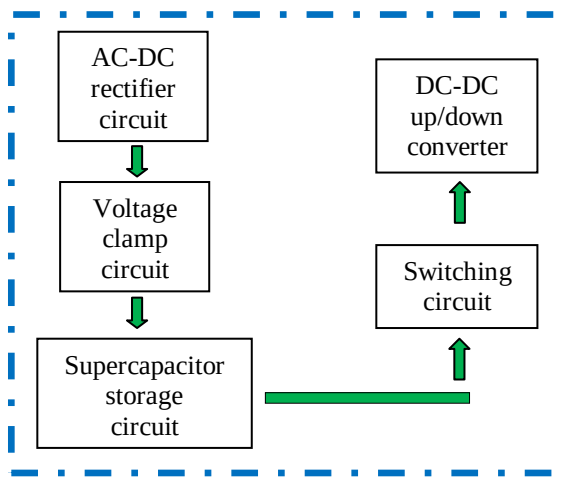

Figure 3: Block diagram of the power management circuit.

Figure 4 shows the lab scale fabricated power management circuit. The schematic design of the power management circuit is designed by using LT Spice software which simulated the performance result. The performance of the power management circuit is measure on the efficiency of the circuit. The efficiency of the power management circuit can be measured based on the Equation (9).

$$Efficiency = \left(\frac{P_{cap}}{P_{source}}\right)(100) = \left[\left(\frac{V_{cap}{}^{2}}{R_{cap}}\right) \div \left(\frac{V_{source}^{2}}{4(R_{source})}\right)\right]100 \quad (9)$$

Where P_{cap} is the power stored inside the supercapacitor (Watt), P_{Source} is the power output from hybrid energy harvester (Watt), V_{cap} is the voltage of the supercapacitor (Volt), R_{cap} is the load resistor at the supercapacitor (Ohm), V_{source} is the voltage of the hybrid energy harvester (Volt) and R_{source} is the resistor at the hybrid energy harvester (Ohm).

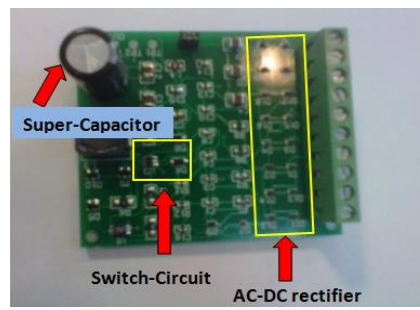

Figure 4: Lab scale fabricated board power management circuit.

Microcontroller and sensors module

The IOIO microcontroller for android phone is a development board for android application that can communicate to the hardware. It features a PIC microcontroller which acts like a bridge that connects an app on our PC or android device to low-level peripheral like GPIO, PWM, ADC, I2C, SPI and UART. A switch on the board can be used to force the IOIO-OTG into host mode, but most of the time the board can be left in 'auto' mode and it will detect its role in the connection.

This 3 axis accelerometer sensor is ADXL335 from Analog Devices. The ADXL335 is a triple axis MEMS accelerometer with extremely low noise power consumption with 320 µA current. The sensor has a full sensing range ±3g. The breakout board comes with on-board 3.3V voltage regulator; therefore it supports voltage range from 2.5 V to 6 V. The board comes fully assembled and tested with external components installed.

The temperature sensor uses a thermistor to measure ambient temperature. The resistance of thermistor changes based on ambient temperature. This resistance value alters the output of a voltage divider which is measured by an analog input pin and converted to a temperature value. The

operating range is -40 to 125° C, with an accuracy of 1.5° C and the operating voltage is from 3.3 V to 5 V.

Part 3: User interface

The last part on the acceleration and temperature condition monitoring system vibration based energy harvesting is the graphical user interface (GUI) with the android application on the phone. Figure 5 shows the GUI on the android phone. The android phone received any signal data of acceleration and temperature sensors through Bluetooth communication from the IOIO microcontroller periodically.

Figure 5: Graphical user interface (GUI) on the android phone.

Acceleration and temperature condition monitoring system

The acceleration and temperature condition monitoring vibration based energy harvesting system is shown in Figure 6. Figure 6 shows the condition monitoring system attached on the vibrating shaker for lab test. The shaker produced the vibration source to the system for harvesting process and source of energy the system. The condition monitoring system data is send to the android phone via Bluetooth dongle. Figure 7 shows the flowchart of this condition monitoring system.

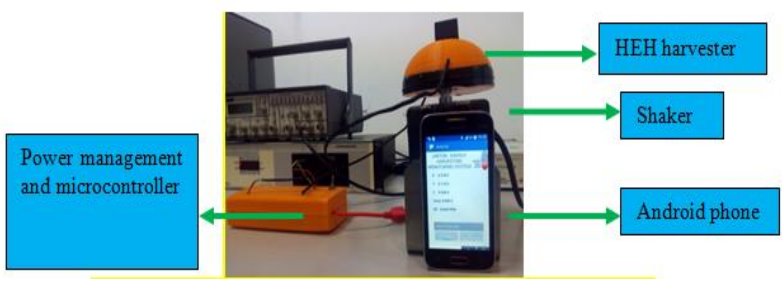

Figure 6: Acceleration and temperature condition monitoring system attached on the shaker.

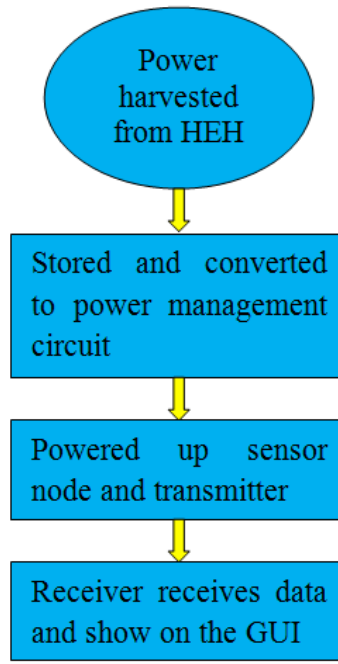

Figure 7: Flowchart of the acceleration and temperature condition monitoring system was tested on vibrating machine.

Power budget for the condition monitoring system

The complete system for the acceleration and temperature condition monitoring system vibration energy harvesting is described above. Table 1 shows the total power budget for the overall system which is 3.83 mJ. A 7000 mF capacitor was selected to match the power budget requirement. The next section describes the performance evaluation for the system.

Table 1: Power budget for the overall system with electronics load

Stage	Voltage (V)	Current (I)	Time (s)	Energy (J)
Sensor and bias circuit	5	175 µA	1.20	1.05 mJ
Analoge devices	5	250 µA	1.20	1.50 mJ
Microcontroller (sleep)	9	0.16 µA	3.24	4.67 µJ
Microcontroller (active)	9	4.1 µA	3.04	0.11 mJ
Wireless devices	5	78 µA	3.00	1.17 mJ
	Total (joules)			3.83 mJ

Measurement results

The experiment setup is shown in Figure 8. The input frequency of the experiment setup was set at function generator from 0 until 100 Hz and the acceleration is controlled at the function generator and amplifier to operate at the 0.25g ms^{-2}. The open circuit voltage was measured at every frequency change by sweeping the frequency at the function generator from 0 Hz to 100 HZ. The laser vibrometer was used to measure vibration level and Labview software was used to log the data. The rectified DC voltage and the charging time were measured at the supercapacitor. The ratio of the power ouput from the supercapacitor storage circuit to the power input from the HEH was calculated as the efficiency of the power management circuit. Another experiment was conducted to observe the ability of the system to transmit signals data from the sensors to the GUI at android phone by harvesting energy from the vibration. Digital multimeter was used to measure the electrical signal. Two multimeters were used to measure the voltage and current at the storage supercapacitor circuit.

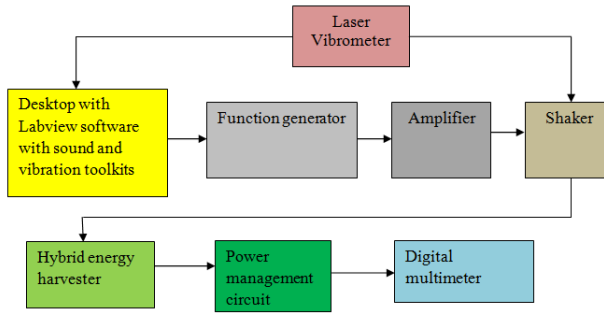

Figure 8: Experimental setup of the acceleration and temperature condition monitoring vibration energy harvesting system.

Power output of HEH

The optimal resistive load of the hybrid energy harvester (HEH) for a given frequency is the one which maximizes the average power output and was identified by tuning the load resistor. The maximum power obtained for different resistors (load) at different frequencies of the HEH was calculated. The experiment was set the frequency sweep from 0 to 100 Hz, but the focus was at the 50±2 Hz. The maximum power output obtained is shown in Table 2. The maximum output power of the HEH harvester is at 50 Hz of resonance frequency with 3.03 mW power output. The test setup is shown in Figure 8.

Table 2: Maximum power output obtained from the HEH harvester

Frequency (Hz)	Optimal resistive load (Ω)	Max. Output Power (mW)
48	220k	2.71
49	217k	2.98
50	200k	3.03
51	180k	2.95
52	230k	2.80

Charging time and voltage output of the supercapacitor storage circuit

The charging time for supercapacitor to fully charge was conducted in the laboratory experiment. The test was conducted to measure the comparison of the charging time with different frequency. The result is shown in Table 3. The charging time was set at 50±2 Hz with 40 Hz and 60 Hz. The charging times are different at the different frequency at 50±2 Hz and charging time are closed to zero for frequency at 40 Hz and 60 Hz. The Table 3 shows at 50±2 Hz the supercapacitor have enough energy to fully charge at different voltage and enough energy to transfer energy to transfer to the electronic load

application and triggered the wireless devices. The test set-up circuit is shown in Figure 9.

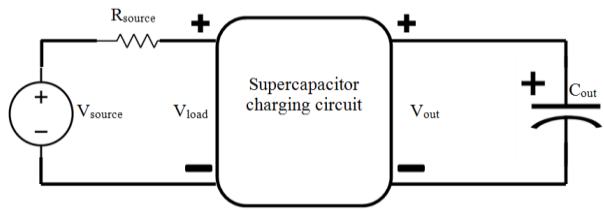

Figure 9: Charging time at supercapacitor charging circuit test set-up.

Table 3: Supercapacitor charging time at different frequency

Frequency (Hz)	Charging time (s)	Voltage at supercapacitor (V)
40	0	0
48	280	11
49	230	15
50	130	18
51	250	12
52	310	10
60	0	0

Power management circuit efficiency

The power transfer efficiency was measured as function of output voltage. This relationship and test set-up for the different frequency at supercapacitor charging circuit is shown in Figure 10. The calculation of the power transfer efficiency is shown in Equation (9). The result is shown in Table 4. The test was set at 50Hz resonance frequency, 200 kΩ load resistor and different input power. This circuit was analyzed at 3 power levels, 500 µW, 1 mW, 2 mW, 2.5 mW and 3.0 mW. These power levels were the minimum expected source power range from HEH. The power levels were realized by the 16 V supply after rectified. The efficiency of the supercapacitor storage circuit in power management circuit reached 85% when the input power of the circuit (from HEH) was 3.0 mW with the power losses around 0.45 mW.

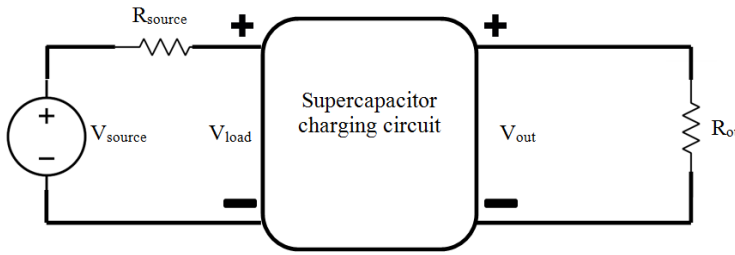

Figure 10: Power transfer efficiency test set-up.

Table 4: Power transfer efficiency

Input Power	Output power	Efficiency
500 µW	200 µW	40%
1 mW	0.46 mW	46%
2 mW	1.1 mW	55%
2.5 mW	1.75 mW	70%
3.0 mW	2.55 mW	85%

Android Graphical user interface (GUI)

The experimental setup is as shown in Figure 11. The result is to observe the ability of the condition monitoring system to power up the system and send data to the android phone. The android phone is enabled to receive data signal from the sensors and microcontroller. The test is repeated several times to observe the ability of the system to power up condition monitoring system from the energy harvesting. The result is shown in Figure 12 and 13. Figure 12 shows the status before and after the condition monitoring system power up from vibration based energy harvesting of the GUI on the android phone.

Figure 13 shows the process of charging and discharging of the supercapacitor storage circuit. Based on the Figure 13, when the supercapacitor is charging the sensors are OFF and when the supercapacitor start to discharge the sensors are ON. This status was measured by connecting the supercapacitor and DC-DC converter with the digital oscilloscope. The graph ON and OFF of Figure 13 is measured to check the initial charge time for supercapacitor and recovery at 8.2 V when the supercapacitor start to supply the power storage to the electronic load application device through DC-DC converter device in power management circuit. The supercapacitor took 130 seconds from 0 V to 10 V for initial charging. The duration for discharge was 5 seconds and it took 15 seconds to recharge again when it was discharged at 8.2 V. Therefore, the data on the android application was updated every 15 seconds.

The DC-DC converter produces 5 V DC to power up electronic load application devices. The 5 V DC start reduce to 0 V when the supercapacitor discharged and reached 8.2 V, the switching circuit (comparator) inside the power management circuit start to cut off the flow of power to the DC-DC converter. The Figure 14 also shows the graph of charge and discharge of supercapacitor voltage with 5 V DC voltage ON and OFF.

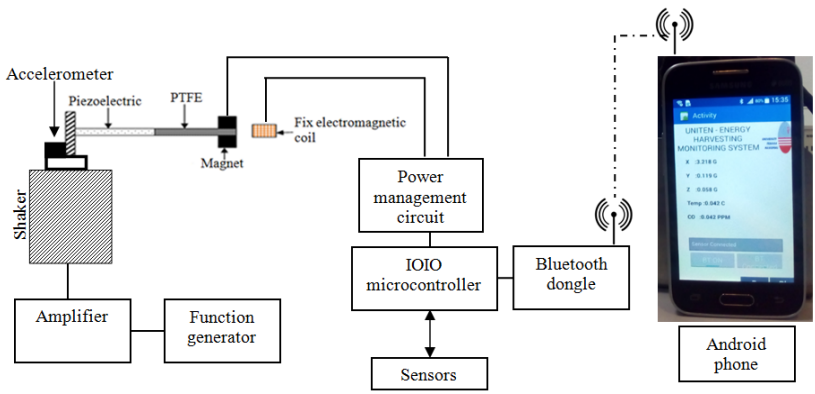

Figure 11: Experimental set-up for the condition monitoring system with the android phone.

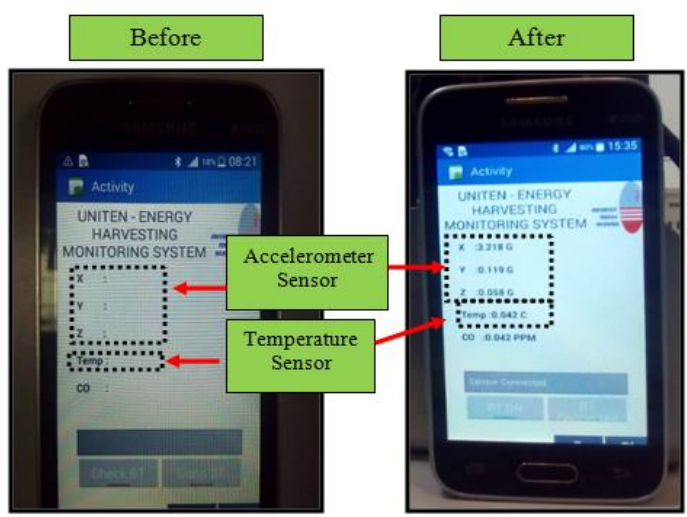

Figure 12: Condition monitoring system status on the android phone.

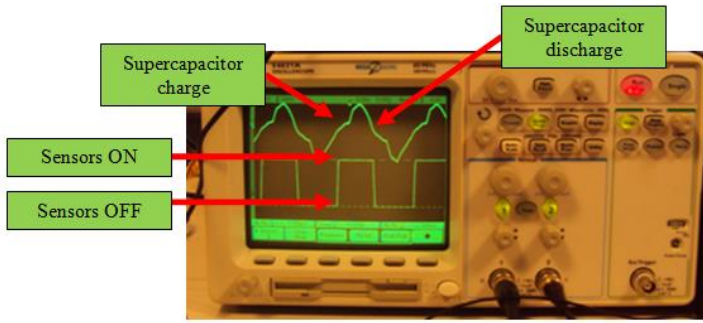

Figure 13: Supercapacitor charging and discharging process with the sensors status.

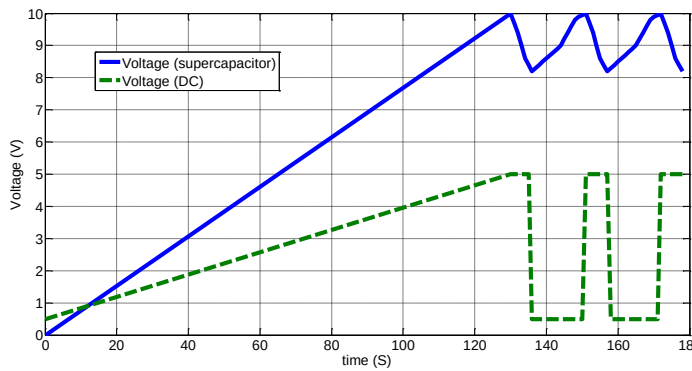

Figure 14: Duration of supercapacitor charging and discharging process related to the sensors status.

Performance comparison

Table 5 shows the comparison of the condition monitoring system of this work with other researchers. This work proposed the system of condition monitoring powered by hybrid energy harvester. In this work, the energy harvester has better output power when compared to Jae Hyuk Jang et al. [27] and L. Chen et al. [28] works. Other previous works of condition monitoring system is powered by using a battery. The range of transceiver is short compared to the other previous works because of the limitation of the Bluetooth technology. This project aims for the monitoring is to transfer data through Bluetooth for android phone application.

Table 5: Performance comparison with other researchers

	This work	[27]	[28]	[43]	[44]
Target application	Condition monitoring	Condition monitoring	Condition monitoring	General wake-up receiver	General WSN
VDD (V)	10	0.93-1.0	7.5	0.5	1.4
Power sources	Hybrid harvester	PZT	PZT	Battery	Battery
Power input	3.00 mW	100µW	NA	Battery	Battery
Power consumption	2.55 mW	1.2 mW	Not mentioned	52 µW	2.6 mW
Wireless communication	Bluetooth	WSN (85 nodes)	WSN	WSN	WSN
Acceleration	0.25g ms^{-2}	0.45g ms^{-2}	0.9g ms^{-2}	NA	NA
Frequency	50 Hz	40.5 Hz	44 Hz	NA	NA
Range of distance	0 - 10 meters	>10 meters	>10 meters	>10 meters	>10 meters

Conclusion

The wireless acceleration and temperature condition monitoring system using android application is presented in this paper. This condition monitoring system is self-powered from the vibration based energy harvester and eliminates the power source from battery. The main challenge in the energy harvesting power source is the low power output. This condition monitoring system operated with autonomous ON and OFF based on the power produced. This condition monitoring system was tested experimentally to operate at resonance frequency of 50±2 Hz and acceleration of 0.25g ms^{-2}. The maximum output power from the hybrid energy harvester was 3.00 mW and the efficiency of the power management circuit was 85% at 2.55 mW power output. At maximum power, initial charging duration of the supercapacitor was 130 seconds, and duration for recharging to 8.2V was 15 seconds. Therefore, the self-powered system managed to transmit data to the android application 15 seconds interval.

Acknowledgement

This research was supported by the Fundamental Research Grant Scheme (FRGS) 20140133FRGS from the Ministry of Higher Education

References

[1] K. Lu, "Materials in Energy Conversion, Harvesting, and Storage," first ed., *John Wiley and Sons*, United State of America, pp. 285–302, (2014).

[2] L. Beker, H.N. Ozguven, H. Kulah, "Optimization of An Energy Harvester Coupled to a Vibrating Membrane," *in: 17th Int. Con. on Solid-State Sensors, Actuators and Microsystems,* pp. 1663–1666, (2013).

[3] Hannan et al., "Energy Harvesting for The Implantable Biomedical Devices: Issues and Challenges," *BioMedical Engineering OnLine*, (2014).

[4] A.S.M. Zahid Kausar, Ahmed Wasif Reza, Mashad Uddin Saleh, and Harikrishnan Ramiah, "Energizing wireless sensor networks by energy harvesting systems:Scopes, challenges and approaches," *Renewable and Sustainable Energy Reviews*, 38. 973–989. (2014).

[5] Raquib Md. Ferdous, Ahmed Wasif Reza and Muhammad Faisal Siddiqui, "Renewable Energy Harvesting for Wireless Sensors Using Passive RFID Tag Technology: A Review," *Renewable and Sustainable Energy Reviews*, 58. 1114–1128, (2016).

[6] Saptarshi Das, Hadi Salehi, Yan Shi, Shantanu Chakrabartty, Rigoberto Burgueno, and Subir Biswas, "Towards packet-less ultrasonic sensor networks for energy-harvesting structures," *Computer Communications*, 101, 94–105, (2017).

[7] Farouq Aliyu and Tarek Sheltami, "Development of An Energy-Harvesting Toxic and Combustible Gas Sensor for Oil and Gas Industries," *Sensors and Actuators B* 231, 265-275, (2016).

[8] S. Bradai, S. Naifar, T. Keutel, O. Kanoun, "Electrodynamic Resonant Energy Harvester for Low Frequencies and Amplitudes", *in: IEEE International Instrumentation and Measurement Technology Conference*, pp. 1152–1156 (2014).

[9] S.D. Kwon, J. Park, K. Law, "Electromagnetic Energy Harvester with Repulsively Stacked Multilayer Magnets for Low Frequency Vibration*," Smart Mater. Struct*. 22 (5) pp.1–12 (2013).

[10] C. Lee, D. Stamp, N.R. Kapania, J.O. Mur-Miranda, "Harvesting Vibration Energy Using Nonlinear Oscillations of An Electromagnetic Inductor," in: *Energy Harvesting and Storage: Materials, Devices, and Applications*, Proc. of SPIE. 7683, 76830Y1-76830Y12, (2010).

[11] T. Galchev, H. Kim, K. Najafi, "A Parametric Frequency Increased Power Generator for Scavenging Low Frequency Ambient Vibrations," *Procedia Chem. 1*, pp. 1439–1442 (2009).

[12] E. Arroyo, A. Badel, F. Formosa, "Energy Harvesting from Ambient Vibrations: Electromagnetic Device and Synchronous Extraction Circuit," *J. Intell. Mater. Syst. Struct.* 24 (16) pp. 2023–2035, (2013).

[13] S. Cheng, W. Naigang, D.P. Arnold, "Modeling of Magnetic Vibrational Energy Harvesters Using Equivalent Circuit Representations," *J. Micromech. Microeng.* 17 (11), pp. 2328–2335, (2007).

[14] G. Sheua, S.M. Yangb, T. Leeb, "Development of A Low Frequency Electrostatic Comb-Drive Energy Harvester Compatible to SoC Design by CMOS Process," *Sensors Actuat. A: Phys.* 167 (1), pp. 70–76, (2011).

[15] P. Basset, D. Galayko, A.M. Paracha, F. Marty, A. Dudka, T. Bourouina, "A Batch Fabricated and Electret-Free Silicon Electrostatic Vibration Energy Harvester," *J. Micromech. Microeng.* 19 (11), pp. 1–12, (2009).

[16] S. Roundy, P.K. Wright, J.M. Rabaey, "A Study of Low Level Vibrations as A Power

Source for Wireless Sensor Nodes," *Comput. Commun*. 26 (11), pp.1131– 1144, (2003).
[17] Y. Suzuki, M. Edamoto, N. Kasagi, K. Kashwagi, Y. Morizawa, "Micro Electrets Energy Harvesting Device with Analogue Impedance Conversion Circuit," *in: Proc. Power MEMS'08*, pp. 7–10, (2008).
[18] G. Despesse, T. Jager, J.J. Chaillout, J.M. L'eger, A. Vassilev, S. Basrour, B. Charlot, "Fabrication and Characterization of High Damping Electrostatic Micro Devices for Vibration Energy Scavenging," *in: Proc. DTIP'05,* pp. 386–390, (2005).
[19] H. Salleh, M. H. Lam, L. Muhamad, M. F. bin Jaafar, "Structural Modification Strategies to Improve Piezoelectric Energy Harvester Performance", *Applied Mechanics and Materials*, Vols. 752-753, pp. 934-940, Apr. (2015).
[20] M. H. Lam, H. Salleh, "PZT Piezoelectric Energy Harvester Enhancement Using Slotted Aluminium Beam", *Advanced Materials Research*, Vol. 1051, pp. 932-936, Oct. (2014).
[21] M. Sofwan M. Resali and Hanim Salleh, "Effect of Rubber Compound Treatment and PTFE Extension Beam on Piezoelectric Energy Harvester Power Density", *Journal of Mechanical Engineering* Vol. SI, No. 2(2), 199-214, (2017).
[22] M. Sofwan M. Resali and Hanim Salleh, "Development of Multiple-Input Power Management Circuit for Piezoelectric Harvester", *Journal of Mechanical Engineering* Vol. SI, No. 2(2), 215-230, (2017).
[23] A.Sh. Kherbeet, Hanim Salleh, B.H. Salman, Mohammed Salim, "Vibration-based piezoelectric micropower generator for power plant wireless monitoring application," *Sustainable Energy Technologies and Assessments*, Volume 11, Pages 42-52, (2015).
[24] E.E. Aktakka, R.L. Peterson, K. Najafi, "Thinned-PZT on SOI Process and Design Optimization for Piezoelectric Inertial Energy Harvesting," *in: 16th Int. Conf. on Solid-State Sensors, Actuators, and Microsystems*, (2011).
[25] H. Durou, G.A. Ardilla-Rodriguez, A. Ramond, X. Dollat, C. Ross, D. Esteve, "Micromachined Bulk PZT Piezoelectric Vibration Harvester to Improve Effectiveness Over Low Amplitude and Low Frequency Vibrations," *in: Proc. Power MEMS*, pp. 27–30, (2010).
[26] K. Morimoto, I. Kanno, K. Wasa, H. Kotera, "High-Efficiency Piezoelectric Energy Harvesters of C-Axis-Oriented Epitaxial PZT Films Transferred Onto Stainless Steel Cantilevers", *Sens. Actuat. A*, 163, 428, (2010).
[27] Jae Hyuk Jang, David F.Berdy, Jangjoon Lee, Dimitrios Peroulis, and Byunghoo Jung, "A Wireless Condition Monitoring System Powered by a Sub-100 μW Vibration Energy Harvester," *IEEE Trans. on Circuits and Systems*., Vol. 60. No. 4, pp. 1082-1093, 2013.
[28] Lijuan Chen,Xiaohui Xu,Pingliang Zeng, and Jianqiang Ma, "Integration of Energy Harvester for Self-Powered Wireless Sensor Network Nodes," *International Journal of Distributed Sensor Networks*, pp.1-7, (2014).
[29] M. G. Tehrani, G. Gatti, M. J. Brennan, D. J. Thompson, and L. Oscillator, "Energy Harvesting from Train Vibrations," *11th Int. Conf. Vib. Probl*., no. September, pp. 9–12, (2013).
[30] M. M. Magdy, N. A. Mansour, A. M. R. F. El-Bab, and S. F. M. Assala, "Human motion spectrum-based 2-DOF energy harvesting device: Design methodology and experimental validation," *Procedia Eng*., vol. 87, pp. 1218–1221, (2014).
[31] S. P. Beeby, M. J. Tudor and N. M. White, "Energy harvesting vibration sources for microsystems applications," *Meas. Sci. Technol.*, vol. 17, no. 12, p. R175, (2006).
[32] P. Li, S. Gao, H. Cai, and L. Wu, "Theoretical analysis and experimental study for nonlinear hybrid piezoelectric and electromagnetic energy harvester," *Microsyst. Technol.*, (2015).
[33] W.-S. Jung, M.-J. Lee, M.-G. Kang, H. G. Moon, S.-J. Yoon, S.-H. Baek, and C.-Y. Kang, "Powerful curved piezoelectric generator for wearable applications," *Nano Energy*, vol. 13, pp. 174–181, Apr. (2015).
[34] T. Huang, C. Wang, H. Yu, H. Wang, Q. Zhang, and M. Zhu, "Human walking-driven wearable all-fiber triboelectric nanogenerator containing electrospun polyvinylidene fluoride piezoelectric nanofibers," *Nano Energy*, vol. 14, pp. 226–235, May (2015).
[35] Paradiso, J.A.; Starner, T., "Energy scavenging for mobile and wireless electronics,"

Pervasive Computing, IEEE, vol. 4, no.1, pp.18-27, Jan.-March (2005).

[36] P. X. Gao, J. Song, J. Liu, and Z. L. Wang, "Nanowire piezoelectric nanogenerators on plastic substrates as flexible power sources for nanodevices," *Adv. Mater.*, vol. 19, pp. 67–72, (2007).

[37] D. G. Dorrell and C. Cossar, "A Vibration-Based Condition Monitoring System for Switched Reluctance Machine Rotor Eccentricity Detection," *IEEE Trans. On Magnetics*, Vol. 44, No. 9, (2008).

[38] J.J. McCullagh, T. Galchev, R.L. Peterson, R. Gordenker, Y. Zhang, J. Lynch, K. Najafi, "Long-Term Testing of A Vibration Harvesting System for The Structuralhealth Monitoring of Bridges," *Sensors and Actuators A*, Vol. 217, pp. 139-150, (2014).

[39] M. Karimi, A.H. Karimi, R. Tikani, S. Ziaei-Rad, "Experimental and Theoretical Investigations on Piezoelectric-Based Energy Harvesting from Bridge Vibrations under Travelling Vehicles," *International Journal of Mechanical Sciences*, (2016).

[40] Minh QuyenLe, Jean-FabienCapsal, MickaëlLallart, YoannHebrard, Andre Van Der Ham, NicolasReffe, LionelGeynet, Pierre-JeanCottinet, "Review on Energy Harvesting for Structural Health Monitoring in Aeronautical Applications," *Progress in Aerospace Sciences*, Vol. 79, pp. 147-157, (2015).

[41] Jae Yong Cho, Sinwoo Jeong, Hamid Jabbar, Yewon Song, Jung Hwan Ahn,Jeong Hun Kim, Hyun Jun Jung, Hong Hee Yoo, Tae Hyun Sung, "Piezoelectric Energy Harvesting System with Magnetic Pendulum Movement for Self-Powered Safety Sensor of Trains," *Sensors and Actuators A*, Vol. 250, pp. 210–218, (2016).

[42] A.S.M. Zahid Kausar, Ahmed Wasif Reza, Mashad Uddin Saleh,Hari krishnan Ramiah, "Energizing Wireless Sensor Networks by Energy Harvesting Systems: Scopes, challenges and Approaches," *Renewable and Sustainable Energy Reviews*, Vol. 38, pp. 973-989, (2014).

[43] N. Pletcher, S. Gambini, and J. Rabaey, "A 52 W Wake-Up Receiver with dBm Sensitivity Using an Uncertain-if Architecture," *IEEE J. Solid-State Circuits*, vol. 44, no. 1, pp. 269–280, Jan. (2009).

[44] D. Daly and A. Chandrakasan, "An Energy-Efficient OOK Transceiver for Wireless Sensor Networks," *IEEE J. Solid-State Circuits*, vol. 42, no.5, pp. 1003–1011, May (2007).

[45] M. Flatscher, M. Dielacher, T. Herndl, T. Lentsch, R. Matischek, J. Prainsack, W. Pribyl, H. Theuss, and W. Weber, "A Bulk Acoustic Wave (BAW) Based Transceiver for an In-tire-Pressure Monitoring Sensor Node," *IEEE J. Solid-State Circuits*, vol. 45, no. 1, pp. 167–177,Jan. (2010).